2003

Superfluorescence Polarization: Signature of Collisional Redistribution

A. Kumarakrishnan

S. Chudasama

Xianming Han
Butler University, xhan@butler.edu

Superfluorescence polarization: Signature of collisional redistribution

A. Kumarakrishnan and S. Chudasama
Department of Physics and Astronomy, York University, Toronto, Ontario, Canada M3J 1P3

X. L. Han
Department of Physics, Butler University, Indianapolis, Indiana 46208, USA

(Received 19 August 2002; revised manuscript received 6 May 2003; published 10 September 2003)

We have studied effects of magnetic sublevel degeneracy on the polarization of superfluorescent pulses generated on the Ca $4s4p\ ^1P_1$–$3d4s\ ^1D_2$ transition at 5.5 μm. These pulses were generated from a cell of length 50 cm by optically pumping calcium vapor on the $4s^2\ ^1S_0$–$4s4p\ ^1P_1$ transition in the presence of Ar gas. The axis of ellipticity of superfluorescence (SF) polarization is oriented parallel to the axis of the pump-laser polarization at large detunings, and undergoes an abrupt rotation through 90° for detunings close to resonance. The distribution of populations in the magnetic sublevels of the $^1P_1$ state can be estimated using a simple model based on previously calculated cross sections for collisionally aided absorption in the presence of an intense (pump) field. For large detunings, these estimates are consistent with the polarized SF intensity measured in the experiment. A direct measurement of the populations of the $^1P_1$ magnetic sublevels also supports the collisional redistribution predicted by the calculated cross sections. We therefore suggest that SF polarization can be a useful signature of collisional redistribution. However, the change in ellipticity is unexpected, and probable causes for this effect are discussed.

DOI: 10.1103/PhysRevA.68.033801 PACS number(s): 42.50.Fx, 42.50.Gy, 42.50.Md

I. INTRODUCTION

It is well known that radiative cross sections for pressure broadened absorption will change substantially in the presence of an intense driving field [1–5]. Radiative transitions associated with scattering processes are modified by quasi-elastic collisions resulting in collisionally aided absorption, and collisional redistribution of pump radiation [6]. If the transition occurs between states with spatial degeneracy, collisional depolarization of scattered radiation also occurs.

In the presence of a strong pump field, radiative excitation is assisted by collisions, and often occurs via a number of pathways dynamically created by the light field. The behavior of the system can be understood in terms of the time scale for the electronic response given as $\tau_c = 1/\Omega'$ where Ω' is the generalized Rabi frequency, and the characteristic binary collision time τ_b. The impact theory of pressure broadened absorption is valid in the weak-field limit when $\Omega'\tau_b \ll 1$. In this case, the perturbation of the atomic system is predominantly by collisions. On the other hand, strong-field effects can be expected to occur when $\Omega'\tau_b > 1$. The field-free or bare atomic levels experience substantial level splittings during the excitation pulse. The magnitude of the level splitting can vary significantly in comparison with the strength of the collisional interaction. In fact, the size of the splitting may be sufficient to affect collisional transfer rates—even to the point of turning certain rates off.

Reference [7] showed that this effect played an important role in state selective excitation based on an analysis of experimental results from a $J=0 \rightarrow J'=1$ (Sr-Ar) system pumped by an intense (100 MW/cm^2) pulsed laser [8]. The collisional transfer rate between the $\Delta m_J = 0$ sublevels coupled by the laser was shown to fall off exponentially as a function of Ω/Δ for $\Omega/\Delta > 1$, while transfer rates to the $\Delta m_J = \pm 1$ sublevels remained relatively large [9]. Here, Ω and Δ are the Rabi frequency and detuning of the pump laser, respectively. This behavior was also confirmed by studies of the polarization of scattered radiation in the same atomic system [10,11].

We present a class of experiments in which the polarization of superfluorescence (SF) is a signature of collisionally assisted population transfer. We have observed SF at 5.5 μm on the Ca $4s4p\ ^1P_1$–$3d4s\ ^1D_2$ transition in a column of calcium vapor buffered with Ar by optically pumping the $4s^2\ ^1S_0$–$4s4p\ ^1P_1$ transition [12] (Fig. 1). SF refers to an initially inverted population evolving from spontaneous emission into a coherent state by coupling through the common electromagnetic field of emitted radiation. The ellipticity of polarization of SF pulses is found to vary abruptly as a function of Ω/Δ. For large detunings ($\Omega/\Delta \leqslant 1$) the axis of ellipticity is oriented parallel to the direction of pump-laser polarization. It switches orientation by 90° for small detunings ($\Omega/\Delta \geqslant 1$).

We explain this effect based on collisionally assisted population transfer to the magnetic sublevels of the $^1P_1$ state, as well as the properties of SF emissions between degenerate atomic states. The SF intensity measured by orient-

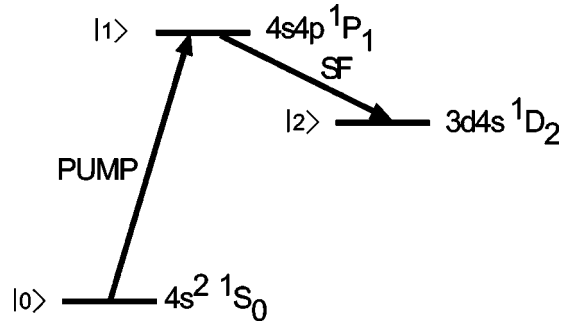

FIG. 1. Ca three-level system; $\lambda_{01} \sim 423$ nm; $\lambda_{12} \sim 5.5$ μm.

ing a polarizer axis parallel and perpendicular to the axis of pump-laser polarization can be related to the populations of the $m_J=0$ and $m_J=\pm 1$ sublevels of the $^1P_1$ state, respectively. For large detunings, estimates for the sublevel populations based on calculated collisional transfer rates [11] can be related to the polarized SF intensity using a simple model. Direct measurements of the $^1P_1$ level populations are also consistent with the predictions of Ref. [11]. But the ellipticity rotation is completely unexpected, and may be due to quantum interference. However, the SF polarization serves as a measure of state selective population transfer, and provides a clear signature of the modification of collision dynamics. The paper is divided into the following sections. Section II describes the collisional redistribution of radiation in a strong field. We discuss the role of optically assisted collisions, which transfer population from dressed states created by the pump laser to the magnetic sublevels of the $^1P_1$ state. In Sec. III, we discuss effects of level degeneracy on SF polarization. Section IV gives a brief description of the experiment, and the results are discussed in Sec. V. Probable causes for ellipticity rotation are discussed in Sec. VI.

II. COLLISIONAL REDISTRIBUTION

We consider a two-level system in which levels $|0\rangle$ and $|1\rangle$ are separated by the atomic frequency ω_{01}. The system is excited by a pulsed laser of frequency ω_L detuned from resonance by $\Delta=\omega_L-\omega_{01}$. The Rabi frequency is given by $\Omega=\vec{p}_{01}\cdot\vec{E}/\hbar$. Here, $\vec{E}$ is the semiclassical field strength, and $\vec{p}_{01}$ is the dipole moment. The generalized Rabi frequency is defined as $\Omega'=(\Omega^2+\Delta^2)^{1/2}$. The duration of a collision with a perturber atom is given by $\tau_b=b_w/v$, where b_w is the Weisskopf radius (an impact parameter which is typically 5–10 Å) that depends on the nature of the potentials describing the interaction, and v is the mean relative velocity of the atoms. The typical duration of a binary collision is $\sim 10^{-12}$ s. For weak fields ($\Omega \ll \Delta$) collisions cause a shift in the energy levels $|0\rangle$ and $|1\rangle$ during the time of interaction. This causes a variation in the frequency of oscillation of atomic dipoles resulting in broadening of the spectral line [13].

Traditionally, the collisional redistribution line shape has been evaluated for two limits of approximation for weak fields.

(i) The impact regime that occurs when the time between collisions T_c is such that $T_c \gg \tau_b$. For this case, the line shape is represented by a Lorentzian profile if $\Delta \ll 1/\tau_b$.

(ii) The quasistatic regime occurs when $\Delta \gg 1/\tau_b$.

Work related to both these limits has been reviewed in detail [14].

Collisional redistribution has been described for the case of strong fields ($\Omega'\tau_b>1$, $\Omega>\Delta$) in Refs. [1–5,15]. This regime produces some unusual effects (see Ref. [6] for a review) such as an intensity-dependent variation for cross sections to undergo collisional transfer (first observed in Ref. [16]). We present a brief outline of these results based on a physical description given by Yeh and Berman [17].

For weak fields, the interaction potential is termed either attractive or repulsive depending on whether collisional shift brings levels $|0\rangle$ and $|1\rangle$ in Fig. 1 closer or farther apart. For an attractive potential, the laser frequency ω_L can be instantaneously in resonance (at an internuclear separation R_c) with the shifted frequency of the atom only for "red" detunings $\Delta<0$. For strong fields, the levels avoid one another due to the interaction caused by the ac Stark shift, and this system can be conveniently described in terms of dressed states [18].

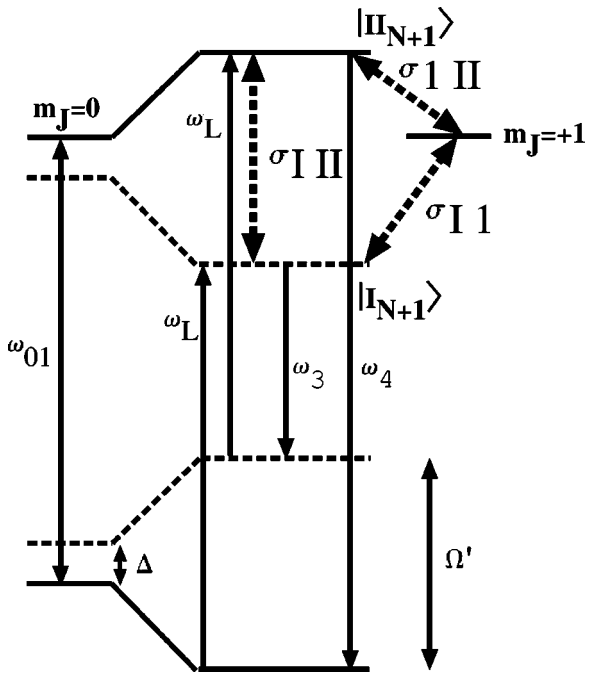

FIG. 2. Dressed states for $\Delta<0$; the doublets are separated by Ω'; ω_L is the laser frequency; ω_3 and ω_4 are frequencies for three- and four-photon processes; $\sigma_{\mathrm{I\,II}}$, $\sigma_{\mathrm{I\,1}}$, and $\sigma_{\mathrm{1\,II}}$ label cross sections for collisional transfer described in text.

Figure 2 shows energy levels of the system for a red detuning. The eigenfunctions of the Hamiltonian

$$H=H_{atom}+V_{atom\text{-}perturber}+H_{field}+H_{int} \tag{1}$$

with

$$\langle 1,N-1|H_{int}|0,N\rangle=-\vec{p}_{01}\cdot\vec{E} \tag{2}$$

are the dressed states of the system. Here, $N(\gg 1)$ represents the number of photons in the laser field. The states consisting of a ladder of doublets (each separated by Ω') can be calculated by using degenerate perturbation theory. The states are given by

$$|\mathrm{I}_N\rangle=\left[\frac{\Omega'(t)+\Delta}{2\Omega'(t)}\right]^{1/2}|0,N\rangle+\left[\frac{\Omega'(t)-\Delta}{2\Omega'(t)}\right]^{1/2}|1,N-1\rangle, \tag{3a}$$

$$|\mathrm{II}_N\rangle=\left[\frac{\Omega'(t)-\Delta}{2\Omega'(t)}\right]^{1/2}|0,N\rangle+\left[\frac{\Omega'(t)+\Delta}{2\Omega'(t)}\right]^{1/2}|1,N-1\rangle. \tag{3b}$$

The dressed states are linear combinations of the atom field states $|0,N\rangle$ and $|1,N-1\rangle$. If $\omega_L \sim \omega_0$, the atom field state $|1,N-1\rangle$ is nearly degenerate with the state $|0,N\rangle$. In this case, the collisional shift of the dressed state $|1,N\rangle$ will be the same as that of the atomic state $|0\rangle$.

If $\Omega \gg \Delta$, the doublets are separated by $\sim\Omega$ and the dressed states in Eq. (3) have equal contributions from the states $|0,N\rangle$ and $|1,N-1\rangle$. Therefore, their relative shift during the collision is zero. The resonances in the weak-field case correspond to avoided crossings between the dressed states (for all detunings). The level splitting at the avoided crossing is proportional to Ω. The cross section for collisional transfer of populations between dressed states is dependent on both Ω and Δ and is defined as

$$\sigma_{\mathrm{I\,II}}(\Omega,\Delta)=\int_0^\infty P_{\mathrm{I\,II}}(b,\Delta,\Omega)2\pi b db. \tag{4}$$

Here, $P_{\mathrm{I\,II}}$ is the transition probability between dressed states I and II for a collision with an impact parameter b. When the duration of the excitation pulse is long compared to the collision time (as in this experiment), a perturber with $b<R_c$ encounters two avoided crossings during the collision. In this case, $P_{\mathrm{I\,II}}$ can be shown to be [15]

$$P_{\mathrm{I\,II}}=(2e^{-z})(1-e^{-z}). \tag{5}$$

Here, e^{-z} is the probability of jumping between interaction potentials at an avoided crossing [19–21], and z is the Landau-Zener parameter given by

$$z=\frac{\pi\Omega^2}{2v(r=R_c)\left(\dfrac{\partial V(r)}{\partial r}\right)_{r=R_c}}. \tag{6}$$

In Eq. (6), $V(r)$ is the atom-perturber potential, and $v(r)$ is the relative velocity between the atom and perturber. R_c is the internuclear separation where the avoided crossing occurs.

At high intensities, $P_{\mathrm{I\,II}} \rightarrow 2e^{-z}$ and the probability for collisional transfer falls off exponentially. This is analogous to the exponential falloff for the probability of tunneling through a potential barrier of width Ω [22]. For an attractive van der Waals potential [15], such an avoided crossing between the dressed states can occur at laser intensities of $\sim$10 MW/cm^2. At low intensities, when z is small, $P_{\mathrm{I\,II}} \rightarrow z$, and hence the probability increases linearly with laser intensity. Thus, the functional form for the cross section for collisional transfer between dressed states will have the shape shown in Fig. 3 [6].

In this work, collisional transfer of populations occurs between the dressed states I and II in the presence of a linearly polarized pump field. Collisional transfer can also occur between the dressed states and the $m_J=\pm1$ sublevels of the $^1P_1$ state which are not coupled to the laser field (Fig. 2). After the turnoff of the pump field, the distribution of populations in the magnetic sublevels of the $^1P_1$ can be predicted if the cross sections for collisional transfer are known.

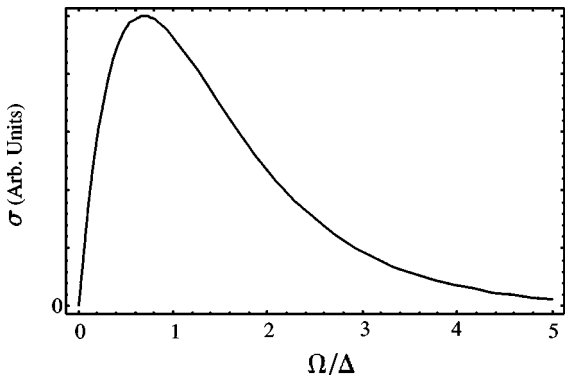

FIG. 3. Typical shape of cross section for collisional transfer as a function of Ω/Δ.

A numerical evaluation of these cross sections was undertaken by Light and Szoke [9] for Sr ($5s^2\,{}^1S_0$–$5s5p\,{}^1P_1$ transition) perturbed by Ar using an attractive van der Waals potential. Although their results were qualitatively similar to the predictions of the Landau-Zener model discussed in this section, they were more accurate for large impact parameters. At high field strengths, they showed that $\sigma_{\mathrm{I\,II}}$ (associated with population transfer to the $m_J=0$ level) falls off sharply for $\Omega/\Delta \geqslant 1$ while the cross sections $\sigma_{\mathrm{I}\pm1}$ (associated with $m_J=\pm1$ levels) remain appreciable for $\Omega/\Delta \geqslant 2$. This was because of the smaller internuclear separations at which avoided crossings occurred for the $m_J=0$ level.

Results of refined calculations of these cross sections [11] are qualitatively similar to the results in Ref. [9]. It was shown [11] that the populations of $m_J=0$ and $m_J=\pm1$ levels due to collisionally aided transitions can be described by simple rate equations for excitation by an adiabatic square pulse. This work also showed that $\sigma_{\mathrm{I}\pm1}$ ultimately falls off for large field strengths. In addition, the cross section $\sigma_{\pm1\,\mathrm{II}}$ for transfer between the $m_J=\pm1$ levels and the dressed state II was evaluated. The effect of this cross section is to equalize populations between the $m_J=0$ and $m_J=\pm1$ levels after the field turns off. These predictions were confirmed by resonance fluorescence experiments [10,15,23,24].

For large detunings, the populations of the magnetic sublevels can be modeled based on the steady-state population of the dressed levels [8,25], the collisional cross sections [11], and the duration of the excitation pulse. Following Refs. [8,25], the population of the dressed level $|1,N+1\rangle$ is given by

$$N_I=\left(\frac{N_0}{2}\right)\frac{\Omega^2}{\Omega^2+\Delta^2}, \tag{7}$$

where N_0 is the ground-state population. The populations transferred by collisions during an adiabatic square pulse of duration τ_P to the $m_J=0$ and $m_J=\pm1$ levels can be written as

$$N_{m=0}=N_{\mathrm{I}}(n_P\sigma_{\mathrm{I\,II}}v)\tau_P, \tag{8a}$$

$$N_{m=\pm1}=N_I(n_P\sigma_{\mathrm{I}\pm1}v)\tau_P, \tag{8b}$$

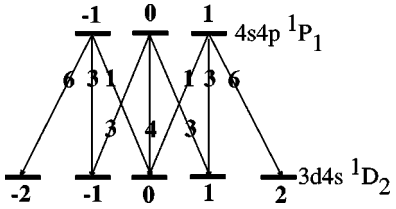

FIG. 4. Ca SF transition showing magnetic sublevels and $[3-j]^2$ coefficients.

respectively. Here, N_P is the perturber (Ar) density. The cross section $\sigma_{\pm 1\,\mathrm{II}}$ is not expected to play an appreciable role in this experiment since SF begins to evolve immediately after the pump-laser turns on. Although the cross sections for the Ca-Ar system can be expected to be smaller than for Sr-Ar [26,27], we note that Eq. (8) can be used for estimating the ratios of populations in the magnetic sublevels used to describe our results. This simple model clearly shows that the population of the $m_J=0$ level is dominant for $\Omega/\Delta<1$ and that the $m_J=\pm 1$ levels are preferentially populated for $\Omega/\Delta>1$.

In addition to collisionally aided absorption, stimulated three- and four-photon processes at ω_3 and ω_4, respectively (Fig. 2), can alter the population of the $m_J=0$ level, especially at small detunings [28]. Other effects that can modify the populations of the magnetic sublevels include radiation trapping, and resonant dipole collisions. Thus the model has to be considerably modified in this case. However, our results pertain mainly to the off-resonance case, for which a simple model based on cross sections in Ref. [11] can be used.

III. POLARIZATION EFFECTS IN SF

Figure 4 shows the nine different SF transitions between magnetic sublevels of the $^1P_1$ and $^1D_2$ states. It is necessary to understand the scaling laws for SF, and competition effects associated with degenerate SF transitions in order to relate the polarized SF intensity to the populations of the magnetic sublevels of the $^1P_1$ state.

SF is characterized by an intense, highly directional burst of radiation at the atomic frequency ω_{12} and a time delay τ_D (usually measured from the onset of the pump pulse) in which the coherence builds up from spontaneous emission. Scaling laws predicted in Ref. [29] for SF peak heights, pulse widths, and delay times were confirmed in Refs. [12,30,31].

The scaling laws can be quantified in terms of the propagation time through the medium $\tau_E L/c$ and the dipole coupling time $\tau_R=1/N\Gamma\mu$. Here, L is the sample length, N is the number of participating atoms, Γ_{12} is the spontaneous emission rate for the SF transition, and μ is a geometrical factor which defines the diffraction solid angle of the interaction volume. If the entire sample is excited at the same time (for example, a transversely excited atomic beam), SF can evolve over a length L only if $\tau_E<\tau_R$ [32]. This would enable atoms at one end of the sample to communicate with atoms at the other end during the evolution of the system. This yields an upper limit for the number of atoms which can participate in cooperative emission. In this case, the SF peak intensity is $\propto N^2$ and the pulse width and time delay (τ_D) are $\propto 1/N$.

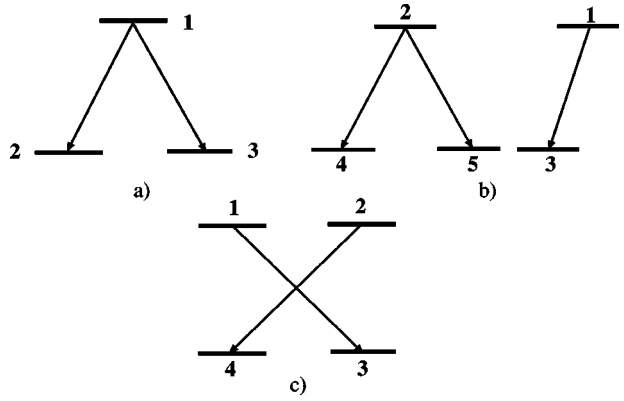

FIG. 5. Competition effects in SF.

On the other hand, if $\tau_E>\tau_R$, we can follow Ref. [29] and consider the column of length L to be divided into S noninteracting slices, each of which emits cooperatively. The emission from the sample can be treated as an incoherent sum of these emissions. As a result the peak intensity is $\propto N$. Each slice of length L_c contains N' atoms such that $S=L/L_c=N/N'=\tau_{R'}/\tau_R$. Here, the dipole coupling time in each slice satisfies the condition $\tau_{R'}=L_c/c$. The number of slices can then be expressed as $S=(\tau_E/\tau_R)^{1/2}$. For this proposition to hold, the evolution time of each slice is $\tau_{R'}=(\tau_R\tau_E)^{1/2}$. The SF pulse width for the entire sample can be shown to scale as $1/N^{1/2}\Gamma_{12}$ and the delay time being proportional to $\tau_{R'}$ scales as $1/N^{1/2}$.

In this work, the sample is excited longitudinally, and the conditions resemble swept excitation. In this case, no upper limit is expected for the number of atoms participating in cooperative emission. However, the Rabi frequency associated with the intense pump pulse modifies the evolution of SF. As a result, the scaling laws predicted for SF in a transversely excited system are valid [12]. For large detunings, the number of slices in the column is of the order of unity and the SF peak intensity is $\propto N^2$. For small detunings, $S>1$ and the peak intensity $\propto N$ (see Fig 4 in Ref. [12]). Thus, changes in the scaling law for the peak intensity as function of detuning have to be taken into account to interpret our results.

Theoretical studies of effects for degenerate transitions and their effects on SF polarization are addressed in Refs. [33,34]. Some of these predictions have been verified experimentally in a series of papers Refs. [35–37]. A summary of these effects (see Fig. 5) which depend on the initial populations of the levels, transition probabilities, and polarization selection rules is given below.

In Fig. 5(a), SF emissions $1\rightarrow 2$ and $1\rightarrow 3$ have a common upper level and their transition rates are such that $\Gamma_{12}>\Gamma_{13}$. In this case, SF on the $1\rightarrow 2$ transition is dominant. Emission on this transition enhances the branching ratio and the $1\rightarrow 3$ transition is suppressed. The SF polarization will be determined by the selection rules for the transition $1\rightarrow 2$. Figure 5(b) shows transitions $2\rightarrow 4$ and $2\rightarrow 5$ which have orthogonal circular polarizations such that $\Gamma_{25}>\Gamma_{24}$. In this

situation, the SF polarization will be determined by the $2 \rightarrow 5$ transition. If however, an independent transition $1 \rightarrow 3$ sets up a field with the same polarization as the $2 \rightarrow 4$ transition (before SF evolves from level 2), then the transition $2 \rightarrow 4$ is favored. In Fig. 5(c), levels 1 and 2 start with equal populations. Transitions $1 \rightarrow 3$ and $2 \rightarrow 4$ have orthogonal circular polarizations and $\Gamma_{13} = \Gamma_{24}$. The SF polarization in this case is expected to be linear for a single realization of the experiment. The direction of linear polarization will fluctuate randomly for each repetition, and the output will be unpolarized if the results are averaged [34]. All these predictions have been verified experimentally [35–37].

The situation in Fig. 5(c) was later reexamined [29] for SF occurring on a $J = 1/2 \rightarrow J' = 1/2$ transition. Let the quantization axis $\hat{z}$ be along the direction of emission. If the substates of the upper level are incoherently excited, and have identical populations at $t = 0$, the output is a sum of two independent emissions which have opposite circular polarizations. In general, emitted pulses will have a random-phase difference, and unequal time delays, and therefore, a time varying polarization. The average value of the difference in delay times is given as $1.3\tau_R$ based on a mean-field model. This difference is typically 30% of the width of each pulse. Since there is a fairly good overlap at the peak of the emission, the same linear polarization will be measured for each repetition of the experiment.

The mean-field model assumes that quantum fluctuations are uniform throughout a slice at the time of initiation, and ignores changes in the values of the atomic polarization, electric field, and number density within the slice during the evolution of SF. Fully quantum-mechanical propagation theories [38] in contrast assume that atoms within a slice are subject to differing local environments during SF initiation and account for changes in the values of physical quantities mentioned above during the evolution. They predict fluctuations in delay times, peak heights, and pulse shapes. As a result, the SF polarization for the system in Fig. 5(c) will be elliptical. The direction of the major axis of the ellipse fluctuates from shot to shot, so that the emission will be unpolarized on averaging [29]. This effect has been observed [36,37]. Studies of SF in Ca [12] showed that the SF delay times are in accord with predictions of a fully quantum-mechanical propagation theory [38]. Mean-field theories significantly underestimate the time delays.

Based on discussions in Secs. II and III, it can be expected that for large detunings, the $^1P_1$ $m_J = 0$ level will be preferentially populated by the linearly polarized pump-laser (see Fig. 4). The SF output will then consist of two contributions. First, the polarization of SF from the $^1P_1$ $m_J = 0$ level will be determined by the dominant $^1P_1$ $m_J = 0 \rightarrow {}^1D_2$ $m_J = 0$ transition (Fig. 4). The emission on this transition will be polarized linearly in the direction parallel to the axis of the pump-laser polarization for each repetition of the experiment. Second, the SF pulses from the $^1P_1$ $m_J = \pm 1$ levels (which still have a significant population) will consist of two opposite circularly polarized emissions on the dominant transitions, namely, $^1P_1$ $m_J = 1 \rightarrow {}^1D_2$ $m_J = 2$ and $^1P_1$ $m_J = -1 \rightarrow {}^1D_2$ $m_J = -2$. The circularly polarized emissions will result in elliptical polarization for each repetition of the experiment. The axis of the ellipse will vary randomly from shot to shot. The combined SF emission will be elliptically SF. The major axis of the ellipse will be oriented parallel to the axis of the pump-laser polarization.

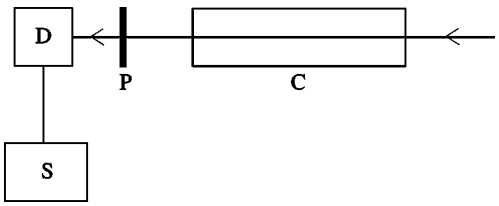

FIG. 6. Schematic of experiment; *C*, cell with Ca and Ar; *P*, polarizer; *D*, Detector; *S*, oscilloscope.

For small detunings, $^1P_1$ $m_J = \pm 1$ levels will be preferentially populated (Fig. 4). The intensity of the linearly polarized contribution from the $m_J = 0$ level will be reduced and the intensity of the randomly polarized contribution from the $m_J = \pm 1$ levels will be much higher. The major axis of the ellipse will again be oriented parallel to the axis of pump-laser polarization.

IV. EXPERIMENTAL DETAILS

The Ca column was longitudinally pumped by pulses from a multimode (1–2 GHz bandwidth) homemade dye laser focused through a 50-cm-long cell containing Ca vapor and a buffer gas (Ar). The confocal beam parameter was comparable to the cell length. A schematic of the experimental setup is shown in Fig. 6. The Ar pressure was measured by a capacitance manometer calibrated to 0.2%. The cell was maintained at a uniform temperature (± 2 °C).

The dye laser was pumped by a frequency tripled (355 nm) commercial yttrium aluminum garnet laser with a repetition rate of 10 Hz. The excitation pulses had a Gaussian spatial profile, a full width at half maximum of 6 ns, and an average pulse energy of 1.25 mJ as measured with a thermopile calibrated to $\pm 2\%$. The pump-laser intensity was ~ 50 MW/cm^2. The peak Rabi frequency was estimated for the pump transition to be $\Omega \sim 20$ cm^{-1}, based on spatial profile measurements. The uncertainty in Ω was $\pm 25\%$.

The pump-laser was tuned to the vicinity of the $^1S_0$-$^1P_1$ transition at 423 nm. It was vertically polarized ($>99\%$) at the entrance of the cell. A small portion of this pulse was incident on a photodiode (rise time ~ 1 ns) which triggered a digital oscilloscope capable of sampling at 1 GS/s. SF at 5.5 μm was imaged directly onto a liquid-N_2-cooled gold doped germanium detector after passing through a Ge filter (without the aid of any mirrors or lenses). Apparatus to measure the SF polarization (wire grid polarizer, MgF_2 wave plate) were placed between the Ge filter and the detector. This detector had a bandwidth of ~ 200 MHz. Its response was also connected to the oscilloscope.

The peak height and area under the pump pulse were held constant to within 10% during the experiment. To measure the SF polarization, the wire grid polarizer was rotated through 360° in regular increments. The transmitted value of the SF intensity was measured by averaging a few hundred

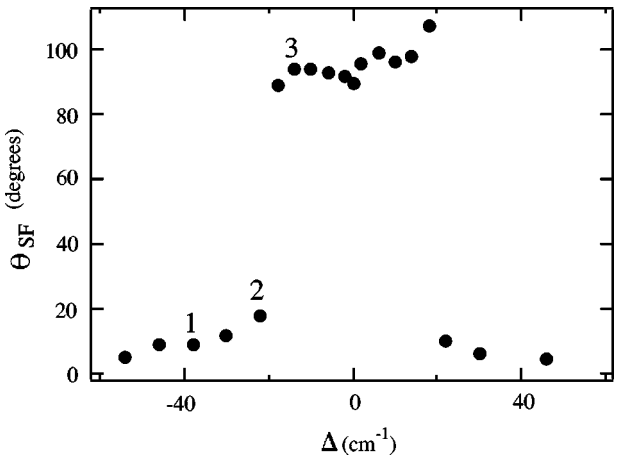

FIG. 7. θ_{SF} vs Δ; $\Omega = 20$ cm^{-1} ($\pm 25\%$); $P_{\mathrm{Ar}} = 1$ Torr; Ca[$^1S_0$] $\sim 3\times 10^{14}$ cm^{-3}.

repetitions. This measurement was repeated as a function of the pump-laser detuning. The polarized SF intensity was also measured by varying the pump-laser intensity and Ar pressure.

The duration of the pump pulse (12 ns) is of the same order as the natural lifetime of the $^1P_1$ level ($T_1 = 4.6$ ns [39]), and the dephasing time of the SF transition ($T_2 \sim 7$ ns) [12]. The branching ratio for the decay from $^1P_1$-$^1S_0$ is $\sim 10^5$ times larger [40] than the decay from $^1P_1$-$^1D_2$ (the radiative rate for the SF transition Γ_{12} has been measured to be 3.68×10^3 s^{-1} [41]; the lifetime of the metastable $^1D_2$ state is ~ 1 ms [42]). The SF delay time varies from ~ 50 ns for large detunings to ~ 12 ns for small detunings, i.e., $\tau_D > T_1$. SF can occur with high efficiency (quantum yield of the order of unity was measured in Ref. [12]) even for long delay times because radiation trapping at the pump wavelength preserves the column of excited states. The Ca $^1S_0$ density was typically $\sim 1\times 10^{14}$ cm^{-3}.

V. DISCUSSION OF RESULTS

Figure 7 shows the angle of ellipticity of SF polarization θ_{SF} as a function of pump-laser detuning Δ at a fixed laser intensity ($\Omega \sim 20$ cm^{-1}). The angle of ellipticity was determined from the transmission function of the polarizer. For each value of Δ, the polarizer was rotated through 360° in increments of 30°. For a given polarizer orientation, the SF intensity I_{SF} was measured by averaging 256 repetitions. The transmission was fit to the form

$$I_{SF} = A\cos^2(\theta) + B, \tag{9}$$

where θ is the polarizer angle measured with respect to the axis of polarization of the pump-laser (defined to be at 0°). The angle for maximum transmission is θ_{SF}. In general, the SF can be elliptically polarized. The quantities $A+B$ and B represent the major and minor axes of the ellipse, respectively. The quantity A represents the modulation amplitude and is a measure of linear polarization along the polarizer axis, whereas B can have contributions from emissions which are linearly polarized perpendicular to the polarizer axis, as well as from emissions which have circular or random polarization.

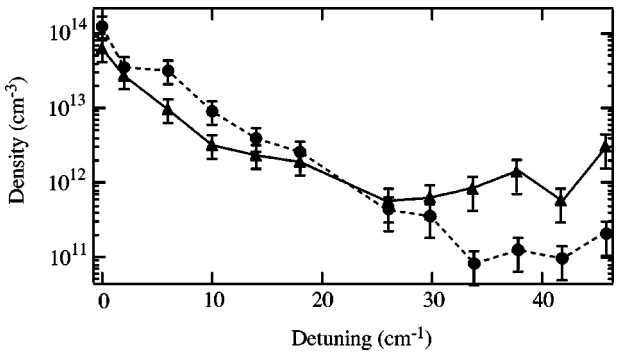

FIG. 8. $^1P_1$ level populations vs Δ for conditions similar to Fig. 7; $m_J = 0$ (triangles), $m_J = \pm 1$ (circles). Points have been joined to aid the eye; $\Omega = 22$ cm^{-1} ($\pm 25\%$); Ca[$^1S_0$] $\sim 3\times 10^{14}$ cm^{-3}.

From Fig. 7, we see that for large $|\Delta|$, the major axis of the ellipse is nearly parallel to the direction of the pump-laser vertical polarization. The reason for the gradual change in θ_{SF} from 0° is not understood. The axis of ellipticity switches abruptly to an orthogonal direction, an effect that is completely unexpected. According to discussions in Secs. II and III, we would expect $\theta_{SF} = 0°$ for all detunings. Only the modulation amplitude A in Eq. (9) was expected to be reduced when the population of the $m_J = \pm 1$ levels becomes dominant at small detunings.

It can also be seen that the change in ellipticity occurs at nearly identical detunings on either side of resonance. It was verified that these results were not limited by the discrimination of the polarizer. The results were unchanged if the polarizer was replaced by a MgF_2 Rochon prism. Points labeled 1, 2, and 3 in Fig. 7 have transmission functions given by $I_{SF} = 270\cos^2(9.0°) + 140$, $I_{SF} = 78\cos^2(18°) + 372$, and $I_{SF} = 679\cos^2(94°) + 415$, respectively. For small $|\Delta|$ such as for the point labeled 3, the SF peak intensity is $\propto N$, and the statistical variation in θ_{SF} determined from fits is $\sim \pm 1°$. The repeatability of data was poor for detunings at which the SF ellipticity changes abruptly such as for the point labeled 2. For large $|\Delta|$ (point labeled 1), the SF peak intensity is $\propto N^2$ and the statistical variation in θ_{SF} is $\sim \pm 2°$. The fits thus reveal a clear change in the SF polarization vs Δ.

In order to verify the predictions for collisional redistribution discussed in Sec. II, we have measured the populations of the magnetic sublevels of the $^1P_1$ state as a function of Δ for a fixed pump-laser intensity. These measurements involved scanning a second pulsed dye laser (probe) across the $4s4p\,^1P_1 \rightarrow 4p^2\,^1S_0$ transition and measuring the absorption. The absorption was generally measured immediately after the turnoff of the pump laser. For the case when the SF delay time was ~ 50 ns, the absorption was measured both immediately after the pump pulse and just before the SF pulse. In all of these cases, the absolute density of the magnetic sublevels was inferred using the method of equivalent widths [43].

The population measurements are shown in Fig. 8. These measurements were obtained at the same ground-state den-

sity and buffer gas pressure as in Fig. 7 and nearly the same Rabi frequency. The results show that the $m_J=\pm 1$ population is clearly larger than the $m_J=0$ population for $\Delta < 15\ \mathrm{cm}^{-1}$. For $\Delta > 25\ \mathrm{cm}^{-1}$, the $m_J=0$ population becomes dominant. The value of the detuning at which the ellipticity rotation occurs in Figs. 7 and 8 is consistent with the values of the Rabi frequency.

It can also be observed that the $m_J=0$ population increases for $\Delta > 35\ \mathrm{cm}^{-1}$. It has been conclusively established that this effect is attributed to SF cascade emissions that populate (primarily) the $m_J=0$ level as a result of two-photon excitation to the $4s10s\ ^1S_0$ transition [44]. The two-photon resonance occurs when the pump-laser is detuned 65.8 cm^{-1} above the $4s^2\ ^1S_0$–$4s4p\ ^1P_1$ transition [44]. It is notable that the SF cascades consist of pulses of duration ~ 1 ns and occur with relatively high efficiency. These SF emissions evolve with time delays of only a few nanoseconds. We have also confirmed on the basis of numerical simulations that three-photon excitation of the $m_J=0$ level cannot model the increase in $m_J=0$ population observed in Fig. 8.

The population measurements support the prediction that the $m_J=\pm 1$ population will be dominant for small detunings as discussed in Sec. II. Although the ellipticity rotation is not explained, it seems reasonable to associate this effect with the preferential excitation of the $m_J=\pm 1$ levels. The probable causes of ellipticity rotation will be discussed in Sec. VI.

We note that it is not possible to obtain accurate estimates for the polarized SF intensity from the population measurements because of the errors associated with the equivalent width technique. Nevertheless, it is possible to compare the polarized SF intensity to predictions based on the cross sections for collisionally aided absorption.

We now consider the average SF intensities I_{90} and I_0 to be indirect measures of the populations of the $m_J=\pm 1$ and $m_J=0$ levels, respectively. Here, I_{90} and I_0 correspond to polarizer orientations perpendicular and parallel to the axis of the pump-laser polarization, respectively. They can be determined from fits to the polarizer transmission function described by Eq. (9). Hence we can write

$$\frac{I_{90}}{I_0}=\left(\frac{N_{m=\pm 1}}{N_{m=0}}\right)^q\left(\frac{6}{4}\right). \tag{10}$$

The populations of the magnetic sublevels N_m affected by collisional transfer can be estimated using Eq. (8). Here, q is an empirically determined quantity ($q=1$ or $q=2$) depending on the scaling law for the SF peak intensity, which varies as a function of pump-laser detuning [12]. The quantity 6/4 is the ratio of $[3-j]^2$ coefficients for dominant SF transitions out of the $m_J=\pm 1$ and $m_J=0$ levels as discussed in Sec. III.

Figure 9 shows a plot of the SF polarization ratio I_{90}/I_0 as a function of Δ for the data in Fig. 7. Its value increases smoothly from ~ 0.3 at large detunings to ~ 2 at small detunings ($I_{90}/I_0=1$ when the SF ellipticity rotates). The data also show a decrease in this ratio to ~ 1.5 in the vicinity of resonance. These results are qualitatively consistent with direct measurements of the populations of the magnetic sublevels discussed earlier. The predictions for the polarization ratio based on the model used in Eq. (9) are shown as the solid line. These predictions appear to be accurate for large detunings. The model predicts a high degree of state selective excitation of the $m_J=\pm 1$ levels for small detunings, since it assumes that the $m_J=0$ level is populated only by collisionally aided absorption. For small detunings, the data are clearly not in agreement with these predictions. This is attributed to the role of multiphoton processes, in particular the three-photon process (see Fig. 2), that can populate the $m_J=0$ level (more effectively at small detunings), and cause the polarization ratio to decrease.

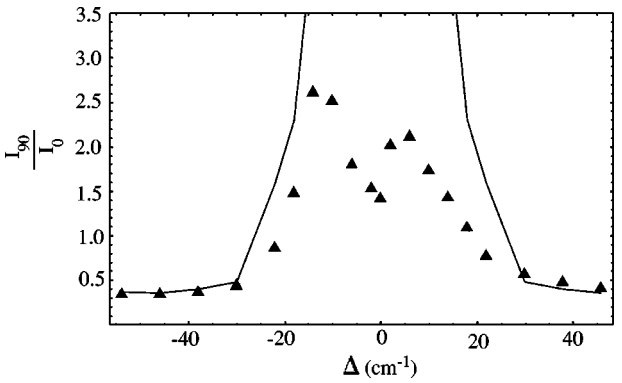

FIG. 9. SF polarization ratio I_{90}/I_0 versus Δ for data in Fig. 7; solid line is prediction based on Eqs. (8) and (10).

We have also carried out a more sensitive test of the predictions of Eq. (10) for large detunings by measuring the value of the detuning (Δ_{flip}) at which the SF ellipticity rotates ($I_{90}/I_0=1$) as a function of the pump-laser intensity I. The SF peak intensity is $\propto N^2$ in this regime. The data shown in Fig. 10 can be fit to the functional form $\Delta_{flip}=17.4I^{0.5}$, which is represented by the solid line. The errors in the parameters of the fit are $\sim \pm 5\%$. This result can be anticipated because for $\Delta > \Omega$, the cross sections $\sigma_{\mathrm{I\,II}}$ and $\sigma_{\mathrm{I}\pm 1}$ both scale linearly with the Rabi frequency Ω.

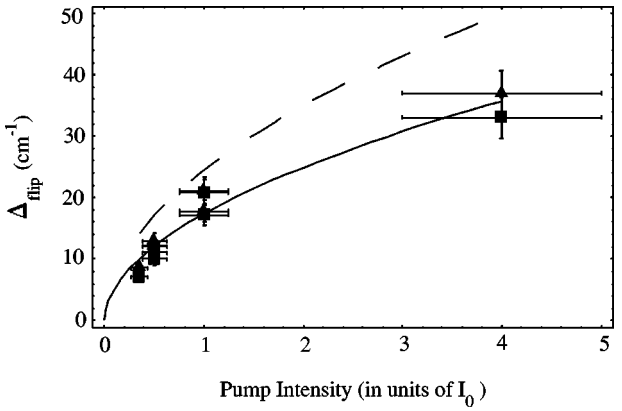

FIG. 10. Δ_{flip} vs pump-laser intensity I; I_0 corresponds to $\Omega \sim 20\ \mathrm{cm}^{-1}$; $P_{\mathrm{Ar}}=1$ Torr; triangles correspond to detunings $\omega_L > \omega_o$; squares correspond to detunings $\omega_L < \omega_o$; solid line is fit to data; dashed line is fit to prediction based on calculated cross sections for collisional transfer. The solid line and the dashed line show the same power-law dependence.

It is significant to note that the expression for Δ_{flip} predicted by Eq. (10) (dashed line) using the calculated cross sections for collisionally aided absorption in Ref. [11] can be fit to the expression given by $\Delta_{flip}=24.5I^{0.5}$. The errors in the fit parameters are $\sim\pm 3\%$. Thus the predictions show the same power-law dependence as the fit to the data. The discrepancy is attributed to the role of the three-photon process. This process can efficiently populate the $m_J=0$ level for detunings close to resonance and cause Δ_{flip} to occur at detunings that are smaller than the values predicted by the model.

It is also significant to note that the experiment was repeated under carefully controlled conditions for $\Delta=0$ [12]. The statistical errors associated with the population measurements were minimized, and systematic errors were studied in detail. In this case, the SF polarization ratio was found to be in agreement with the measured distribution of populations in the magnetic sublevels. This agreement suggests that the contributions to the SF intensity due to circularly polarized and randomly polarized emissions must be small. Separate measurements with a quarter wave plate and polarizer showed that the intensity of circular polarization was $<5\%$ of the total SF intensity for the range of detunings in Fig. 9. This result suggests that for $I_{90}/I_0>1$, the SF is dominated by emission linearly polarized perpendicular to the axis of pump-laser polarization.

Apart from collisional redistribution, radiation trapping can also affect the distribution of populations in the magnetic sublevels. We have modeled the effect of radiation trapping (in Ref. [30]). The simulations suggest that the SF delay time τ_D should be appreciably modified if $\tau_D>\tau_N$. Here, τ_D is the natural lifetime of the $^1P_1$ level. However, no such modification was observed in Ref. [12]. Measurements of the density and spatial distribution of the $^1P_1$ level just before the onset of SF at $\tau_D=46$ ns were consistent with the prediction for the expansion of the radiatively trapped column of excited states. However, the ratio of the magnetic sublevel populations was unchanged within experimental error. We therefore conclude that radiation trapping did not appreciably alter the magnetic sublevel populations of the excited state.

Resonant optical dipole collisions between Ca atoms can be expected to modify the ratio of populations in the magnetic sublevels. Although these cross sections can be of the same order of magnitude as the cross sections for collisional transfer, the Ca density was ~ 100 times smaller than the Ar density. We therefore do not expect this effect to modify the scaling law shown in Fig. 10 which was obtained for a detuning range of 10–40 cm^{-1}. The ratio of densities recorded for $\tau_D=46$ ns was the same within experimental error as the ratio measured immediately after the excitation. In addition, the polarization measurements were unchanged when the Ca density was reduced by a factor of 2. These measurements suggest that dipole collisions do not contribute significantly.

In summary, it is clear that SF polarization can provide a clear signature of collisional redistribution. It is also clear that the predictions for the SF polarization have to be improved, particularly for detunings closer to resonance. This can be realized by solving a comprehensive model based on rate equations that describes the population transfer to the $^1P_1$ levels [15]. However, the ellipticity rotation remains unexplained, and probable causes are discussed in the following section.

VI. CAUSES FOR ELLIPTICITY ROTATION

It is possible that the preferred SF polarization at 90° to the axis of pump-laser polarization may be due to an inherent asymmetry. Probable causes could include hyperfine structure and external magnetic fields. Since calcium has no hyper-fine structure, we performed several tests to check the dependence of the ellipticity rotation on magnetic fields. The data were unaltered when the cell heater coils were temporarily shut off (these coils produce a longitudinal magnetic field during the experiment). When the axis of the pump-laser linear polarization was rotated using a half-wave plate at the cell entrance, the major axis of the SF ellipse oriented at 90° was observed to follow the axis of the pump-laser polarization. This test seems to rule out effects associated with the Earth's magnetic field, as well as effects due to the residual magnetization of the stainless steel cell. The characteristics of the ellipticity rotation were identical for SF emissions from both ends of the cell, and the data were not altered if the direction of propagation of the pump-laser through the cell was reversed.

Other causes for this effect could be the presence of a coherence in the medium either due to the pump pulse [45] or due to SF cascade emissions [44]. Coherence due to the pump pulse could result in stimulated Raman scattering (SRS) which occurs at the frequency $\omega_L-\omega_{02}$ (Fig. 2). SRS and SF cascade emissions can be expected to shorten the time delays for SF. No such effects were observed on the SF time delay.

No tunable emission at the SRS frequency was observed in this experiment [12]. If SRS was present, we estimate that its intensity must be at least 500 times smaller than the SF intensity. The SF delay times were in agreement with predictions [38], based on a fully quantum-mechanical model of initiation [12]. Predictions for the shortening of SF delay times based on a mean-field model [45] did not agree with experimental results.

We also note that the axis of ellipticity of SRS polarization is known to undergo a rotation when the pump-laser is tuned in the vicinity of a doublet of atomic states [46]. The ellipticity rotation of SRS has been attributed to effects of quantum interference between two scattering amplitudes involving the doublet and the atomic level on which the stimulated process terminates. A similar effect has also been shown to be responsible for polarization properties of Rayleigh scattering [47,48], two-photon scattering [49], and three-photon scattering [50]. More recently, quantum interference effects have been shown to be responsible for the cancellation of spontaneous emission [51,52].

We therefore speculate that the polarization rotation may be explained only if it can be shown that the spectrum of spontaneous emission is dominated by linearly polarized photons whose axis of polarization is at 90° with respect to the axis of polarization of the pump-laser.

VII. CONCLUSIONS

We have presented a more detailed analysis of a class of scattering experiments in which the polarization of the SF provides a signature of collisional redistribution [53]. The SF polarization ratio I_{90}/I_0 has been found to be consistent with direct measurements of the populations in the magnetic sublevels close to resonance. For large detunings, the polarization ratio is in good agreement with predictions based on previously calculated values of cross sections for collisionally aided absorption.

Since collisional redistribution plays an important role in controlling the rates of chemical reactions, an effective method of monitoring these rates is of value. Since the polarization ratio seems to be insensitive to radiation trapping (as in Refs. [8,10,11]), SF polarization may offer certain practical advantages. Improvements to the reported experiments could include more accurate measurements of sublevel populations using cw diode lasers. It would also be useful to obtain more precise estimates for the Rabi frequency by using a single-mode pump-laser. Related work could include a study of SF polarization using ultrashort pump pulses, which are known to substantially modify the effects of collisional redistribution [54].

ACKNOWLEDGMENTS

These experiments were carried out at the University of Idaho under the guidance of Jim Kelly. A.K. would like to thank Paul Kleiber and Jinx Cooper for helpful discussions on collisional redistribution of radiation. The experimental work was supported by NSF PYI, NSF EPSCOR (Idaho), and AFWL. Subsequent analysis was supported by NSERC, CFI, OIT, PRO, and York University.

[1] L.I. Gudzenko and S.I. Yakovlenko, Zh. Eksp. Teor. Fiz. **62**, 1686 (1972) [Sov. Phys. JETP **35**, 877 (1972)].
[2] V.S. Lisitsa and S.I. Yakovlenko, Zh. Eksp. Teor. Fiz. **66**, 1550 (1974) [Sov. Phys. JETP **39**, 759 (1974)].
[3] V.S. Lisitsa and S.I. Yakovlenko, Zh. Eksp. Teor. Fiz. **68**, 479 (1975) [Sov. Phys. JETP **41**, 233 (1975)].
[4] N.M. Kroll and K.M. Watson, Phys. Rev. A **13**, 1018 (1976).
[5] A.M.F. Lau, Phys. Rev. A **13**, 139 (1976).
[6] K. Burnett, Phys. Rep. **118**, 339 (1985).
[7] A. Szoke, Opt. Lett. **2**, 36 (1978).
[8] J.L. Carlsten, A. Szoke, and M.G. Raymer, Phys. Rev. A **15**, 1029 (1977).
[9] J. Light and A. Szoke, Phys. Rev. A **18**, 1363 (1978).
[10] P.D. Kleiber, K. Burnett, and J. Cooper, Phys. Rev. Lett. **47**, 1595 (1981).
[11] P.D. Kleiber, J. Cooper, K. Burnett, C.V. Kunasz, and M.G. Raymer, Phys. Rev. A **27**, 291 (1983).
[12] A. Kumarakrishnan and X.L. Han, Phys. Rev. A **58**, 4153 (1998).
[13] I.I. Sobelman, L.A. Vainshtein, and E.A. Yukov, in *Excitation of Atoms and Broadening of Spectral Lines*, edited by J. Peter Toennies (Springer-Verlag, Berlin, 1981).
[14] N. Allard and J. Kielkopf, Rev. Mod. Phys. **54**, 1103 (1982).
[15] P.D. Kleiber, Ph.D. thesis, University of Colorado, 1981 (unpublished).
[16] A.M. Bonch-Bruevich, T.A. Vartanyan, and V.V. Khromov, Zh. Eksp. Teor. Fiz. **78**, 538 (1980) [Sov. Phys. JETP **51**, 271 (1980)].
[17] S. Yeh and P.R. Berman, Phys. Rev. A **19**, 1106 (1979).
[18] Y.R. Shen, *The Principles of Nonlinear Optics* (Wiley, New York, 1984).
[19] L.D. Landau and E.M. Lifshitz, *Quantum Mechanics, Non Relativistic Theory* (Pergamon, Oxford, 1977), Chap. 11.
[20] C. Zener, Proc. R. Soc. London, Ser. A **137A**, 696 (1932).
[21] E.C.G. Stueckelberg, Helv. Phys. Acta **5**, 369 (1932).
[22] U. Fano, in *Fundamental Processes of Atomic Dynamics*, edited by J.S. Briggs, H. Kleinpoppen, and H.O. Lutz (Plenum, New York, 1987).
[23] P.D. Kleiber, K. Burnett, and J. Cooper, Phys. Rev. A **25**, 1188 (1982).
[24] P.D. Kleiber, K. Burnett, and J. Cooper, Phys. Lett. **84A**, 182 (1981).
[25] B.R. Mollow, Phys. Rev. **188**, 1969 (1969).
[26] J.M. Farr and W.R. Hindmarsh, J. Phys. B **4**, 568 (1971).
[27] J.J. Wright and L.C. Balling, J. Chem. Phys. **73**, 1617 (1980).
[28] C.H. Skinner and P.D. Kleiber, Phys. Rev. A **21**, 151 (1979).
[29] M. Gross and S. Haroche, Phys. Rep. **93**, 301 (1982).
[30] A. Kumarakrishnan, Ph.D. thesis, University of Idaho, 1992 (unpublished).
[31] A. Kumarakrishnan, J.F. Kelly, and X.L. Han, Bull. Am. Phys. Soc. **38**(3), 1154 (1993).
[32] F.T. Arecchi and E. Courtens, Phys. Rev. A **2**, 1730 (1970).
[33] A. Crubellier, Phys. Rev. A **15**, 2430 (1977).
[34] A. Crubellier and M.G. Schweighofer, Phys. Rev. A **18**, 1797 (1978).
[35] A. Crubellier, S. Liberman, and P. Pillet, Phys. Rev. Lett. **41**, 1237 (1978).
[36] A. Crubellier, S. Liberman, P. Pillet, and M.G. Schweighofer, J. Phys. B **14**, L177 (1981).
[37] A. Crubellier, S. Liberman, and P. Pillet, J. Phys. B **17**, 2771 (1984).
[38] D. Polder, M.F.H. Schuurmans, and Q.H.F. Vrehen, Phys. Rev. A **19**, 1192 (1979).
[39] W.L. Wiese, M.W. Smith, and B.M. Miles, *Atomic Transition Probabilities*, Natl. Bur. Stand. Ref. Data Ser., Natl. Bur. Stand. (U.S.) Circ. No. 22 (U.S. GPO, Washington, D.C., 1969), Vol. II.
[40] N. Beverini, F. Giammanco, E. Maccioni, F. Strumia, and G. Vissani, J. Opt. Soc. Am. B **6**, 2188 (1989).
[41] L.P. Lellouch and L.R. Hunter, Phys. Rev. A **36**, 3490 (1987).
[42] R.N. Diffenderfer, P.J. Dagdigian, and D.R. Yarkony, J. Phys. B **14**, 21 (1981).
[43] A. Corney, in *Atomic and Laser Spectroscopy* (Oxford University Press, Oxford, 1977).
[44] A. Kumarakrishnan and X.L. Han, Opt. Commun. **109**, 348 (1994).

[45] C.M. Bowden and C.C. Sung, Phys. Rev. A **18**, 1558 (1978); **20**, 2033 (1979).
[46] D.C. Hanna, M.A. Yuratich, and D. Cotter, *Nonlinear Optics of Free Atoms and Molecules* (Springer, Berlin, 1979).
[47] G. Placzek, *Handbuch der Radiologie* (Akadedmisches Verlaggesellschaft, Leipzig, 1934), Vol. VI, Pt. 2, p. 209.
[48] A.C. Tam and C.K. Au, Opt. Commun. **19**, 265 (1976).
[49] J.E. Bjorkholm and P.F. Liao, Phys. Rev. Lett. **33**, 128 (1974).
[50] V. Shevy, M. Rosenbluh, S. Hochman, A.D. Wilson-Gordon, and H. Friedmann, Opt. Lett. **13**, 1005 (1988).
[51] S.E. Harris, Phys. Rev. Lett. **62**, 1033 (1989).
[52] H.R. Xia, C.Y. Ye, and S.Y. Zhu, Phys. Rev. Lett. **77**, 1032 (1996).
[53] J.F. Kelly, A. Kumarakrishnan, and X.L. Han, Bull. Am. Phys. Soc. **36**(7), 1953 (1991); A. Kumarakrishnan and X.L. Han, *ibid.* **44**(1), 1641 (1999).
[54] T. Sizer and M.G. Raymer, Phys. Rev. Lett. **56**, 123 (1986).